

# Transmission-mode x-ray magnetic circular dichroism characterization of moment alignment in Tb-doped Ni<sub>81</sub>Fe<sub>19</sub>

Y. Guan and Z. Dios

Department of Applied Physics and Applied Mathematics, Columbia University,  
New York, New York 10027

D. A. Arena

National Synchrotron Light Source, Brookhaven National Laboratory, Upton, New York 11973

L. Cheng and W. E. Bailey

Materials Science Program, Department of Applied Physics and Applied Mathematics, Columbia University,  
New York, New York 10027

(Presented on 10 November 2004; published online 28 April 2005)

We present transmission-mode XMCD characterization of Fe, Ni, and Tb moment alignment in Tb-doped Ni<sub>81</sub>Fe<sub>19</sub> thin films. The use of transmission geometry measurements has allowed the extraction of absolute projected elemental moments in the alloy. A very low projected Tb moment at 6% doping level, which nonetheless reverses with low applied fields (40 Oe), indicates a sperimagnetic alignment with respect to the Fe and Ni elements in the cosputtered polycrystalline alloy. © 2005 American Institute of Physics. [DOI: 10.1063/1.1856732]

## I. INTRODUCTION

Rare-earth (RE) dopants are of growing interest for the control of ultrafast magnetization dynamics. Small concentrations of Tb have been found to enhance the damping factor ( $\alpha$ ) of Ni<sub>81</sub>Fe<sub>19</sub> by orders of magnitude, which is useful to decrease the subnanosecond settling time of switched magnetization states. The contributed damping has been identified with the presence of an orbital moment on the rare-earth dopant.<sup>1</sup>

X-ray magnetic circular dichroism (XMCD) is an ideal technique to characterize the magnetic character of RE dopants, especially in separating orbital and spin moments on different elements in a multicomponent material. Total electron yield (TEY) XMCD has been used previously to confirm the nominal orbital-to-spin moment ratios of Tb and Gd dopants<sup>2</sup> using sum rules. However, total projected moments could not be extracted by TEY, as is typical, due to the surface-sensitivity of the measurement and possible influence of an oxidized surface.

Transmission-mode XMCD<sup>3</sup> is known to be a superior technique for quantitative extraction of total element-specific moments due to its minimal influence from surface oxidized layers, critical for RE species, its absence of yield saturation effects and absence of field-induced background drift. In this article, we have carried out transmission-mode XMCD measurements on Si/Si<sub>3</sub>N<sub>4</sub>(membrane)/(Ni<sub>81</sub>Fe<sub>19</sub>)<sub>1-x</sub>:Tb<sub>x</sub>(100 nm)/Au(3 nm) samples, deposited by UHV cosputtering of Ni<sub>81</sub>Fe<sub>19</sub> and Tb targets on Si<sub>3</sub>N<sub>4</sub> membranes at a base pressure of 10<sup>-9</sup> Torr. We determine that the projected moment fraction of Tb is roughly 8% that of Ni and Fe, indicating noncollinear moment alignment of the rare-earth species.

## II. EXPERIMENT

Tb-doped Ni<sub>81</sub>Fe<sub>19</sub> (100 nm) thin films were grown onto Si/Si<sub>3</sub>N<sub>4</sub>(membrane) substrates using UHV magnetron sput-

tering at a base pressure of 10<sup>-9</sup> Torr. (Ni<sub>81</sub>Fe<sub>19</sub>)<sub>1-x</sub>:Tb<sub>x</sub> doped samples were made by confocal sputtering from Ni<sub>81</sub>Fe<sub>19</sub> alloy and elemental Tb targets under an applied field of 20 Oe.

Tb-doped Ni<sub>81</sub>Fe<sub>19</sub> thin films (100 nm thick), with doping level 0% and 6%, were investigated in the study. All thin films were capped with a thermally evaporated 3 nm Au layer to prevent oxidation before transport to NSLS. The overall film structure is, therefore, [Si/Si<sub>3</sub>N<sub>4</sub> (membrane)/(Ni<sub>81</sub>Fe<sub>19</sub>)<sub>1-x</sub>:Tb<sub>x</sub>(100 nm)/Au(3 nm)]. Film thickness and alloy compositions were monitored by a quartz crystal microbalance and *ex situ* profilometry.

XMCD measurements were taken in transmission mode at the UV ring of the National Synchrotron Light Source (NSLS), Brookhaven National Laboratory, Beamline U4B. XMCD were measured for fixed circular photon helicity, 70% polarization, with pulsed magnetization switching ( $H = \pm 40$  Oe) at the sample; photon incidence was fixed at 45° with respect to the sample normal. The samples were mounted with magnetic easy axis along the applied field directions. U4B at NSLS does not have the capability to reverse the photon helicity in a simple way, which prevents the collection of all four combinations of positive and negative field and helicity which are optimum to avoid the presence of XMCD artifacts. Thus, XMCD measurements with  $H+(M+)$  measured first and  $H-(M-)$  measured second were averaged with measurements taken in reversed order (“duplex mode”), to correct for any drift in the monochromator which might lead to derivativelike artifacts in XMCD. XMCD measurements were divided by the factor  $0.70 \cos 45^\circ$  to correct for nongrazing incidence and incomplete circular polarization. Background spectra  $I_S(\omega)$ <sup>3</sup> from the bare membrane were recorded for each energy interval and applied in the background subtraction.

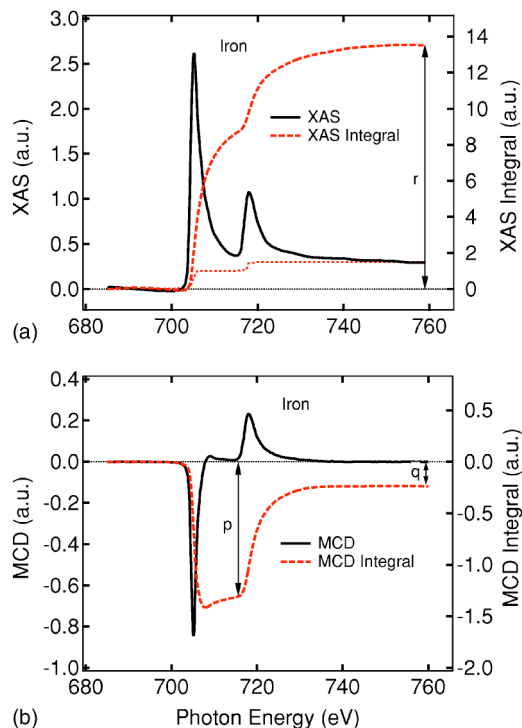


FIG. 1. (Color online)  $L_{2,3}$ -edge XAS and MCD spectra of iron at undoped  $\text{Ni}_{81}\text{Fe}_{19}$  thin film: (a) summed XAS spectra and its integral; (b) MCD spectra and its integral.

### III. RESULTS AND DISCUSSION

Selected results of XMCD characterization of the local magnetization states on Fe, Ni, and Tb are shown in Figs. 1–3. Data analysis needed for the transmission spectra have

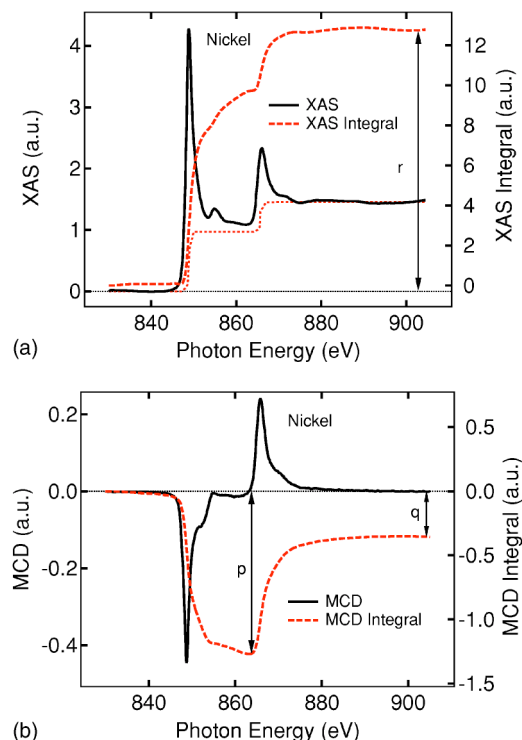


FIG. 2. (Color online)  $L_{2,3}$ -edge XAS and MCD spectra of nickel at undoped  $\text{Ni}_{81}\text{Fe}_{19}$  thin film: (a) summed XAS spectra and its integral; (b) MCD spectra and its integral.

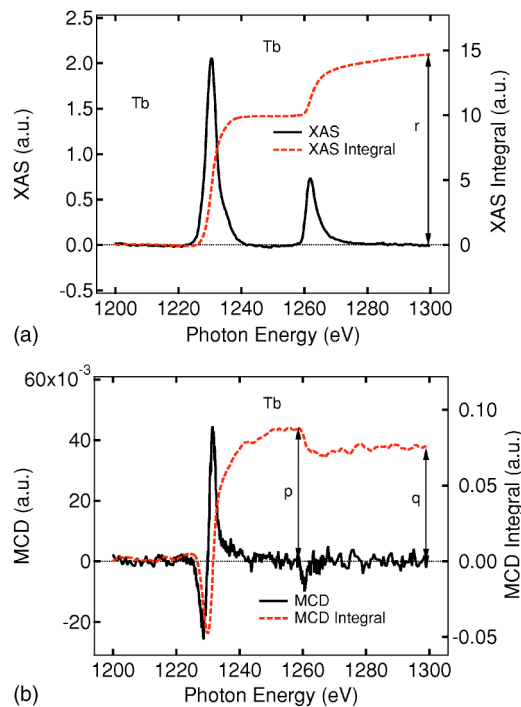


FIG. 3. (Color online)  $M_{4,5}$ -edge XAS and MCD spectra of Tb at 6% Tb-doped  $\text{Ni}_{81}\text{Fe}_{19}$  thin film: (a) summed XAS spectra and its integral; (b) MCD spectra and its integral.

followed the method of Chen *et al.*<sup>3</sup> Sum rules<sup>4,5</sup> have been applied to extract projected orbital, spin, and total magnetic moments of all elements present. In general, the magnitude of elemental moments is proportional to the magnetic circular dichroism (MCD, difference in absorption on magnetization/helicity switching) normalized to the x-ray absorption (XAS, averaged for magnetization switching). Spin and orbital moment ratios are given by the relative weight of MCD at the  $L_3$  or  $M_5$  edge ( $p$ ) to that at the  $L_2$  or  $M_4$  edge ( $q$ );  $r$  denotes XAS above background. At the  $L_{2,3}$  edges of transition metals (e.g., Fe, Ni), orbital and spin moments are given by [neglecting the  $\langle \hat{T}_z \rangle / \langle \hat{S}_z \rangle$  term,  $c=1$ ,  $l=2^5$ ]

$$m_{\text{orb}} = \frac{-4q(10 - n_{3d})}{3r}, \quad m_{\text{spin}} = \frac{-(6p - 4q)(10 - n_{3d})}{r} \quad (1)$$

and at the  $M_{4,5}$  edges of rare-earths (e.g., Tb) [ $c=2$ ,  $l=3^5$ ]

$$m_{\text{orb}} = \frac{2q(14 - n_{4f})}{r}, \quad m_{\text{spin}} = \frac{(5p - 3q)(14 - n_{4f})}{r} \left( 1 + 3 \frac{\langle \hat{T}_z \rangle}{\langle \hat{S}_z \rangle} \right)^{-1} \quad (2)$$

Thus we have for Fe and Ni,  $m_{\text{orb}}/m_{\text{spin}} = 2q/(9p - 6q)$ ; while for Tb,  $m_{\text{orb}}/m_{\text{spin}} = [2q/(5p - 3q)](1 + 3(\langle \hat{T}_z \rangle / \langle \hat{S}_z \rangle))$ .

The MCD and summed XAS spectra and their integrals for Fe and Ni in the undoped  $\text{Ni}_{81}\text{Fe}_{19}$  thin film, are shown in Figs. 1 and 2. The MCD and summed XAS spectra and their integrals for Tb in the 6% Tb-doped  $\text{Ni}_{81}\text{Fe}_{19}$  thin film is

TABLE I. Projected orbital and spin magnetic moments of Fe, Ni in the undoped  $\text{Ni}_{81}\text{Fe}_{19}$  thin film (0%) and those of Fe, Ni, and Tb in the 6% Tb-doped  $\text{Ni}_{81}\text{Fe}_{19}$  thin film (6%). For Fe and Ni, the experimental error bars of the XMCD results are estimated to be 5% for  $m_{\text{orb}}/m_{\text{spin}}$ , and 10% for  $m_{\text{orb}}$  and  $m_{\text{spin}}$ . For Tb, the experimental error bars are estimated to be 40% for  $m_{\text{orb}}/m_{\text{spin}}$ , and 50% for  $m_{\text{spin}}$  and  $m_{\text{orb}}$ .

	Fe(0%)	Fe(6%)	Ni(0%)	Ni(6%)	Tb(6%)
$\langle m_{\text{orb}} \rangle / \langle m_{\text{spin}} \rangle$	0.05	0.02	0.08	0.014	0.54
$\langle m_{\text{orb}} \rangle (\mu_B/\text{atom})$	0.08	0.01	0.06	0.002	0.06
$\langle m_{\text{spin}} \rangle (\mu_B/\text{atom})$	1.78	0.51	0.73	0.15	0.11
$\langle m_{\text{total}} \rangle (\mu_B/\text{atom})$	1.86	0.52	0.79	0.15	0.17

shown in Fig. 3. Compared to the MCD and summed XAS spectra obtained in the TEY mode, higher-quality spectra are obtained here, especially for Fe and Ni.

The Tb MCD spectra obtained here, which shows a net positive peak at  $M_5$  with a smaller negative peak on the low energy side and a small disturbance at  $M_4$ , is consistent with elemental Tb MCD spectra found by van der Laan *et al.*<sup>6</sup>

For Tb, according to atomic calculations done by Jo *et al.*,<sup>7</sup>  $\langle \hat{T}_z \rangle / \langle \hat{S}_z \rangle = -0.08$ . For  $n_{3d}$ , we used elemental values of 6.5 for Fe and 8.5 for Ni. For  $n_{4f}$ , we used an elemental value of 8 for Tb according to  $4f^{Z-57}$ . Using these assumptions, we can determine the  $m_{\text{orb}}$  to  $m_{\text{spin}}$  ratios, as well as the individual  $m_{\text{orb}}$  and  $m_{\text{spin}}$  values for Fe, Ni, and Tb. Results are listed in Table I. We find  $m_{\text{orb}}/m_{\text{spin}}$  estimates of 0.05 for Fe, 0.08 for Ni, in the undoped  $\text{Ni}_{81}\text{Fe}_{19}$  thin film; and of 0.54 for Tb in the 6% Tb-doped  $\text{Ni}_{81}\text{Fe}_{19}$  thin film. These values are in reasonable agreement with those found for elemental Fe and Ni thin films. The Tb result is close to the Hund's value of 0.5; the difference can be attributed to the uncertain value of  $\langle \hat{T}_z \rangle / \langle \hat{S}_z \rangle$  in the alloy. We measure projected spin moments of  $1.78 \mu_B/\text{atom}$  for Fe and  $0.73 \mu_B/\text{atom}$  for Ni in the undoped case. In the 6% doped film, these projected values are reduced to roughly 25% of their undoped values, attributable to our inability to saturate the material at the available field of 40 Oe. The degree of alignment of Tb is far smaller, reaching only roughly 8% ( $0.11 \mu_B/\text{atom}$  for spin moment) that of Fe, Ni at 6% doping level. However, for Tb, the total projected moment is only 2% of its ideal saturated level of  $9.0 \mu_B/\text{atom}$ .<sup>8</sup>

Low levels of dichroism and low projected moment, observed on randomly distributed Tb dopants in polycrystalline  $\text{Ni}_{81}\text{Fe}_{19}$  can be interpreted as an accurate reflection of a small averaged projected moment from Tb sites in the alloy. Based on the experimental results of the low projected Tb moment, which nonetheless reverses with low applied fields, the magnetic state of the alloy thus appears to be sperimagnetic<sup>9</sup> with a strong dispersion angle of Tb moments, nonetheless aligned net antiparallel to Fe and Ni mo-

ments. Much higher applied fields (to several Tesla) will be necessary to test whether saturation moments of Tb can be observed.

#### IV. CONCLUSION

Transmission-mode XMCD has been used to characterize the alignment of elemental moments in Tb-doped  $\text{Ni}_{81}\text{Fe}_{19}$  thin films. Compared with TEY-mode XMCD data, it can obtain greatly improved Fe and Ni XMCD spectra, but a similarly low level of Tb dichroism with identically shaped spectra. The low projected Tb moment, which nonetheless reverses with low applied fields, indicates a sperimagnetic alignment with respect to the Fe and Ni elements in the cosputtered polycrystalline alloy.

#### ACKNOWLEDGMENTS

The authors thank Joe Dvorak (NSLS/U4B) for beam-line support. This work was partially supported by Army Research Office Young Investigator Program (ARO-43986-MS-YIP) and the National Science Foundation Grant (DMR-02-39724). Research was carried out in part at the National Synchrotron Light Source, Brookhaven National Laboratory, which is supported by the U.S. Department of Energy, Division of Materials Sciences and Division of Chemical Sciences, under Contract No. DE-AC02-98CH10886.

<sup>1</sup>S. Reidy, L. Cheng, and W. Bailey, Appl. Phys. Lett. **82**, 1254 (2003).

<sup>2</sup>W. Bailey, H. Song, and L. Cheng, cond-mat 0403627 (2004).

<sup>3</sup>C. Chen, Y. Idzerda, H.-J. Lin, N. Smith, G. Meigs, E. Chaban, G. Ho, E. Pellegrin, and F. Sette, Phys. Rev. Lett. **75**, 152 (1995).

<sup>4</sup>B. Thole, P. Carra, F. Sette, and G. van der Laan, Phys. Rev. Lett. **68**, 1943 (1992).

<sup>5</sup>P. Carra, B. Thole, M. Altarelli, and X. Wang, Phys. Rev. Lett. **70**, 694 (1993).

<sup>6</sup>G. van der Laan, E. Arenholz, Z. Hu, A. Bauer, E. Weschke, C. Schussler-Langeheine, E. Navas, A. Muhlig, G. Kaindl, J. Geodkoop *et al.*, Phys. Rev. B **59**, 8835 (1999).

<sup>7</sup>Y. Teramura, A. Tanaka, B. Thole, and T. Jo, J. Phys. Soc. Jpn. **65**, 3056 (1996).

<sup>8</sup>R. C. O'Handley, *Modern Magnetic Materials: Principles and Applications* Wiley, New York (2000).

<sup>9</sup>J. M. D. Coey, J. Appl. Phys. **46**, 1646 (1978).